

## Full Length Article

## Photon-collection improvement from laser-textured AZO front-contact in thin-film solar cells

D. Canteli<sup>a,\*</sup>, I. Torres<sup>a</sup>, S. Fernández<sup>a</sup>, J.D. Santos<sup>a</sup>, M. Morales<sup>b</sup>, C. Molpeceres<sup>b</sup><sup>a</sup> División de Energías Renovables, Energía Solar Fotovoltaica, CIEMAT, Avda. Complutense, 40, 28040 Madrid, Spain<sup>b</sup> Centro Láser, Universidad Politécnica de Madrid, Carretera de Valencia km 7,3, Madrid 28031, Spain

## ARTICLE INFO

## Keywords:

Laser texturing

Silicon solar cells

Transparent conductive oxides (TCO)

## ABSTRACT

With the objective of increasing light scattering and obtaining a higher light absorption in thin-film solar cells, we have textured aluminum-doped zinc oxide (ZnO:Al) films deposited by RF magnetron sputtering on glass substrates using a nanosecond pulsed laser working at 355 nm. The textures have been achieved by simply patterning the ZnO:Al surfaces through direct scribing, using either a linear pattern consisting of equally separated parallel grooves, or a crisscross pattern obtained by performing a second array of laser scribes perpendicular to the former. The relationship between the light scattering properties of the textured films and its morphology are discussed considering two different scattering sources: the pattern formed by the grooves that works as a diffraction grating, and a random roughness of low amplitude created during the laser process. To further characterize the textured samples, amorphous silicon solar cells were deposited onto ZnO:Al films with different textures and their spectral response and short-circuit current ( $J_{sc}$ ) measured. An increment of 15% in  $J_{sc}$  compared to non-textured solar cells is achieved, with ample room for improvement.

## 1. Introduction

In the photovoltaic industry, laser sources have proven to be a very useful tool for a wide number of applications, including edge isolation, fired contacts, selective doping, monolithic interconnection of cells in modules, material crystallization and surface texturing. Surface texturing is a crucial step in solar cell manufacturing since it can successfully reduce surface reflectance and enhance light scattering in materials to promote light absorption in the device absorber. Depending on the material or the texture sought, the process is usually carried out via chemical etching [1,2], plasma etching [3], e-beam lithography [4], aluminum-induced texturing [5], laser interference [6] or simply through the natural texture obtained in some materials during the deposition process [7].

In addition to the established methods, an increasing interest in the use of lasers for surface texturing has emerged recently as a cleaner and cheaper alternative, and because it can produce textures otherwise not possible with the standard methods. Examples where laser texturing has been successfully used include work on crystalline [6,8,9] or amorphous silicon [10], different wide band-gap semiconductors [11], glass substrates [7] and examples where it is used together with a posterior wet etching [8] or a plasma etching step [10].

In the particular case of laser texturing transparent conductive

oxides (TCOs), some works can be found in direct-laser interference patterning [12,13], but many of the examples available require more complex processes. As an example, Johnson et al. [14] used an excimer laser to anneal aluminum-doped zinc oxide (ZnO:Al) films followed by a chemical etching in a dilute HCl solution to enhance the films optical properties, and Li et al. [15] obtained textured Ni/FTO bilayers by magnetic-field assisted laser irradiation.

Taking into account the extensive use of TCO's in the photovoltaic and electronics industry, the study of new techniques to enhance their properties and applications is clearly interesting. In this work, we present results on laser texturing ZnO:Al films. By creating simple patterns using laser direct scribing over the TCO surface, we manage to increase the light scattering and improve the short-circuit current in solar cells deposited onto the textured substrates by up to 15% compared with the non-textured material. This kind of laser texturing procedure offers several advantages with respect to plasma or chemical etchings. First, it is a considerably cleaner and more environmentally friendly process since neither toxic chemicals are used nor contaminated wastes are produced. In addition, the process is highly selective so one can easily limit the area to be affected without resorting to expensive and contaminating photolithographic processes. And finally, it can be easily translated to a wide range of materials, regardless of the crystallographic structure.

\* Corresponding author.

E-mail address: [david.canteli@upm.es](mailto:david.canteli@upm.es) (D. Canteli).<https://doi.org/10.1016/j.apsusc.2018.08.267>

Received 23 March 2018; Received in revised form 27 August 2018; Accepted 31 August 2018

Available online 01 September 2018

0169-4332/ © 2018 Elsevier B.V. All rights reserved.

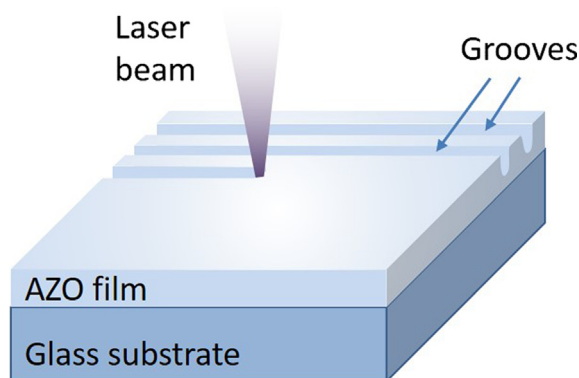


**Fig. 1.** Diagram of the laser texturing process of ZnO:Al thin-films used in this work. Various linear patterns are obtained by direct scribing parallel grooves using different pulse energies, process velocities, and distance between grooves. To obtain a crisscross pattern, a second array of laser processes is scribed perpendicular to the former.

## 2. Experimental

### 2.1. Sample preparation

ZnO:Al films were deposited at a substrate temperature of 350 °C onto 15 × 15 cm<sup>2</sup> Corning 7059 glass substrates by a commercial confocal UNIVEX 450B RF magnetron sputtering system from Oerlikon Leybold Vacuum. The as-deposited ZnO:Al films presented an average transmittance of 81% in the range between 300 and 900 nm, and a sheet resistivity  $R_{\text{sheet}}$  of 3 Ω/□. The films exhibited very smooth surfaces, with a root mean square height ( $S_q$ ) about 7 nm and the thickness was kept constant at about 400 nm.

The ZnO:Al films were textured using a diode-pumped solid-state laser (Nd:YVO4) from Spectra Physics working at the third harmonic wavelength (355 nm). The duration of the laser pulses is about 10 ns and the beam radius on focus is about 17 μm measured at 1/e<sup>2</sup> of the pulse peak fluence. For simplicity, only two different texture patterns were investigated: a simple pattern obtained by scribing parallel grooves with a constant separation between them (see Fig. 1), and a crisscross pattern obtained performing a second array of parallel laser scribes perpendicular to the former ones.

Process speed, laser pulse energy, and distance between lines, were varied to obtain a variety of morphologies, with scribes ranging from widely spaced to overlapping grooves, and from almost undamaged surfaces to scribes that reached the glass substrate (see Fig. 2).

The  $R_{\text{sheet}}$  of the ZnO:Al films increased after the texturing process, more so in the textures produced with deeper scribes where the  $R_{\text{sheet}}$  could reach values as high as several hundred MΩ/□. To ensure the low  $R_{\text{sheet}}$  needed for solar cell operation, an additional 400 nm thick ZnO:Al layer was deposited onto the laser-textured films. With this additional layer, the  $R_{\text{sheet}}$  of all the samples is kept at ~3 Ω/□ while at the same time we ensure that all the samples exhibit a similar surface state, thus making the comparison between the different morphologies easier. As expected [16], the deposition of this second ZnO:Al layer produces a slight smoothening of the surface morphology, leading to a drop of about 4% in the haze factor of the films, regardless of the previous morphology.

Hydrogenated amorphous silicon (a-Si:H) PIN solar cells were deposited onto a selection of textured films. The a-Si:H P-I-N structures were deposited at 250 °C by a MVSystem plasma enhanced chemical-vapor-deposition reactor operating at 13.56 MHz and, after that, 1 cm<sup>2</sup> 200 nm thick aluminum back contacts were deposited by thermal evaporation. Details on the cells deposition can be found in [17].

### 2.2. Characterization techniques

To characterize the textured ZnO:Al samples, we focused on the morphologic, optical and electrical properties. The distance between grooves, their depths, and  $S_q$ , were characterized using a confocal microscope (Leica SensoScan DCM 3D). The optical properties (coherent transmittance ( $T_c$ ) and total transmittance ( $T_t$ )) of the films were measured with a PerkinElmer Lambda 1050 spectrophotometer equipped with a 60 mm integrating sphere. From these spectra, we calculated the haze factor i.e. the percentage of light scattered in the film surface as: Haze factor = 100( $T_t - T_c$ )/ $T_t$ . Finally, the electrical sheet resistance of the films was determined using the four-point-probe method.

In addition to the physical characterization, numerical simulations were performed to understand the mechanisms responsible for the light scattering in the textured surfaces. By using a COMSOL simulation software version 4.4 with a radio frequency module, a model based on the experimental system used to measure the total and diffuse transmittances of the film was constructed. Then, the electromagnetic scattering problem was solved by using the finite element method (FEM) to discretize the Helmholtz equation in space and solve it numerically as a boundary value problem. In order to keep computation time and simplicity in check, a 2D model was used with the experimental profiles of the ZnO:Al samples textured with a linear pattern. The model consisted in a semi-circular domain with the ZnO:Al film in its base. The light enters the system through the ZnO:Al film and scatters in its surface, traveling towards the semi-circular edge where the far-field intensity is calculated as a function of the scattering angle. By integrating far-field intensity it is possible to calculate the specular and diffuse transmittance and the haze factor. Details on the model and the methodology used have been published previously [18].

To study the changes introduced by the textured films in the optical behavior of the solar cells, we measured the spectral response of the a-Si:H solar cells under short-circuit conditions. With these measurements, it is possible to analyze and compare the improvements achieved in the photon collection within the device at different wavelengths. Finally, the short circuit current  $J_{\text{sc}}$  was derived from the spectral response measurements.

## 3. Results and discussion

### 3.1. Light scattering in ZnO:Al laser-textured samples

The capability of the textured ZnO:Al films to scatter incident light was evaluated through the haze factor. The as-deposited ZnO:Al films showed very little surface roughness, with a  $S_q$  ~7 nm and a haze factor of roughly 0%. Likewise, the samples least affected by the laser processes, with  $S_q$  values similar to as-deposited samples, showed also little scattering. But as laser scribes went deeper and the distance between scribes shortened, the  $S_q$  roughness went up to more than 150 nm and the haze factor rose to significant values.

For all the different textures investigated, the haze factor reached its maximum at short wavelengths, decreasing almost linearly as the wavelength further increases. In the case of the linear pattern, the haze factor averaged up to 24% from 350 nm to 600 nm, and up to 13% from 600 nm to 900 nm. In the case of crisscross patterns, those values could ramp up to 34% and 19% respectively.

Table 1 includes the process parameters of four selected samples textured with a crisscross morphology, as well as the  $S_q$  roughness and the haze factor measured at 600 nm.

In Fig. 2 confocal microscopy images of those samples can be seen. To study the effect of the different observed morphologies, the selected samples went from deep scribes that reached the glass substrate (texture T1), to an almost unaffected film, with a cracked surface and little material ablation (texture T4). The measured  $S_q$  values for the four different samples were 138 nm, 85 nm, 71 nm and 30 nm for T1, T2, T3

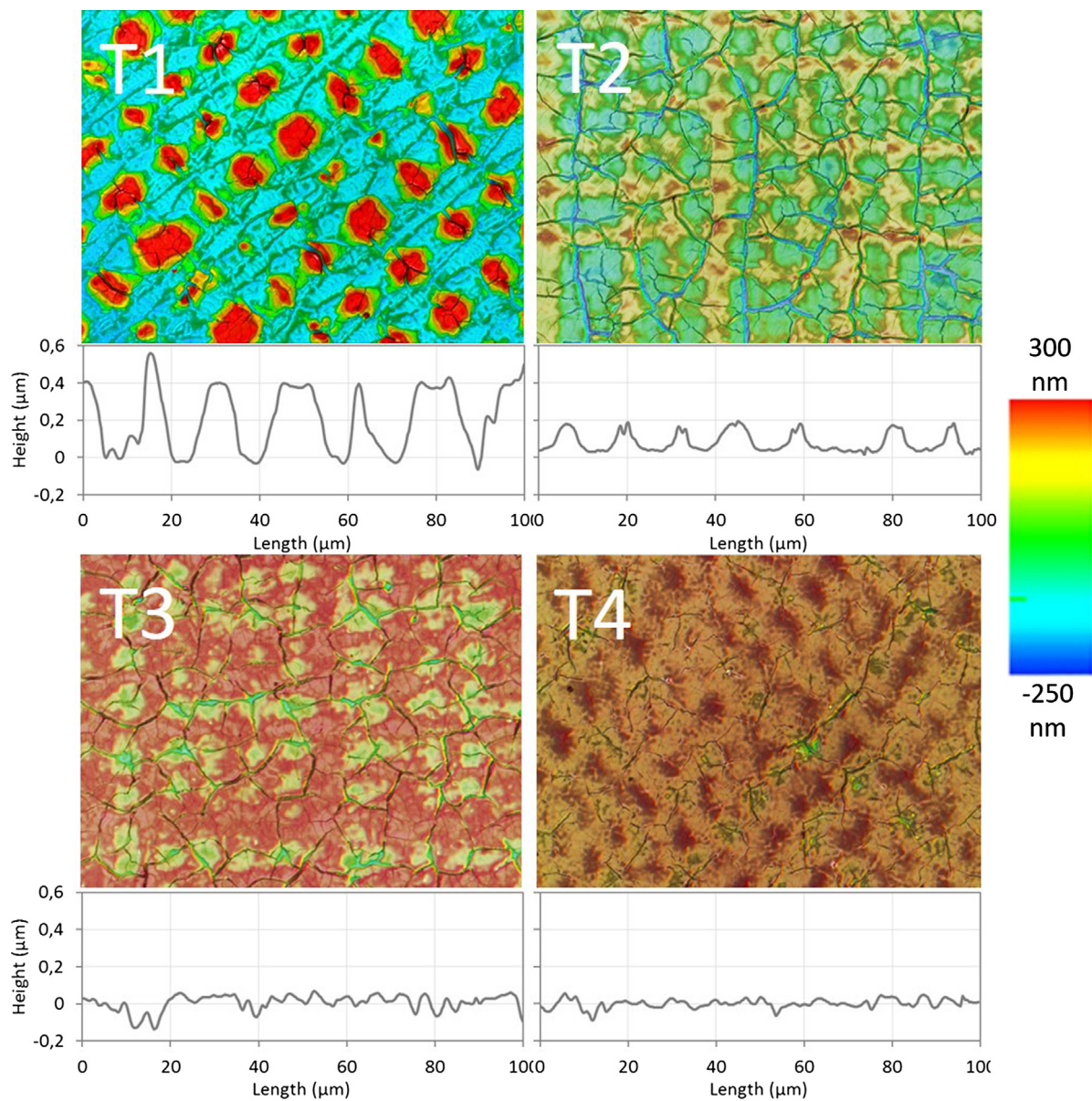


Fig. 2. Confocal microscope images and profiles of four laser-textured ZnO:Al substrates using different process parameters.

**Table 1**  
Process parameters,  $S_q$  roughness and haze factor at 600 nm of the laser-textured AZO selected samples.

Sample	Pulse energy		Pitch $\mu\text{m}$	$S_q$ roughness nm	Haze factor at 600 nm %
	J	%			
T1	$1.9 \cdot 10^{-6}$	95.0	17	138	28.3
T2	$2.3 \cdot 10^{-6}$	85.3	13	85	20.0
T3	$2.1 \cdot 10^{-6}$	70.6	13	71	18.9
T4	$1.9 \cdot 10^{-6}$	70.6	13	30	7.5

and T4 respectively. The haze factor for those samples can be seen in Fig. 3. The same four samples are used in subsection 3.3 as front contacts in a-Si:H-based solar cells, so data for Asahi U-type substrates, a commercial TCO ( $\text{SnO}_2:\text{F}$ ) specifically designed for a-Si:H thin film solar cells operation, is also shown in Fig. 3 to highlight the obtained results.

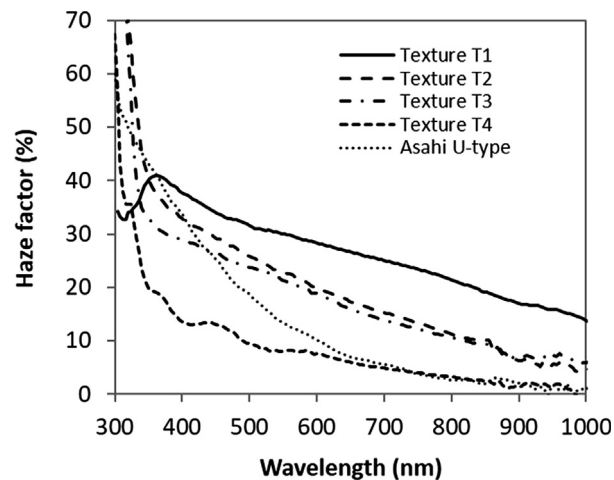


Fig. 3. Haze factor vs wavelength measured for the textured ZnO:Al films shown in Fig. 2 and used for the fabrication of a-Si:H solar cells in subsection 3.3.

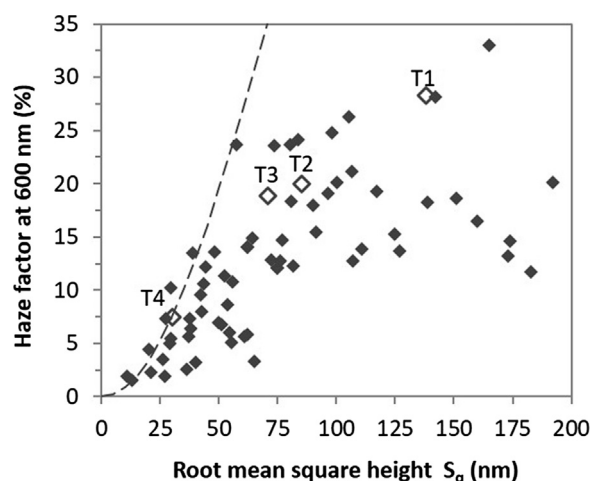


Fig. 4. Haze factor values measured at 600 nm vs  $S_q$  for obtained laser-textured ZnO:Al films. Hollow diamonds correspond to the samples shown in Fig. 2. Dashed line is the best fit according to the scalar scattering theory for random surfaces (see text).

### 3.2. Scattering sources and FEM modeling

The surface morphology of the textured ZnO:Al samples mostly resembles an ordered structure superimposed with a random texture. This is easily observed in parallel patterns, but it can also be appreciated in texture T2 in Fig. 2. Both structures can contribute to the light scattering and need to be evaluated.

In the case of fully random textured surfaces, light scattering is usually studied using the *scalar scattering theory*, which relates the surface roughness to the haze factor through a simple relationship [2,19,20]. This theory, however, is based on two assumptions not fulfilled in the studied samples, namely a totally random roughness and a roughness correlation length much greater than the wavelength of the incident light [19]. Thus, if we apply this theory to a wide set of textured ZnO:Al samples, we can see that the predicted relationship rapidly deviates from the experimental results (see Fig. 4). Although a general tendency of higher haze factor for higher  $S_q$  values is present, there is not a clear relationship between both parameters. Therefore, while the surface random roughness may be a source for light scattering, it does not seem to be the main one.

The second scattering source considered is the structured pattern of laser scribes. When the textured ZnO:Al films are illuminated with a coherent light beam, they behave as a diffraction grating and a pattern of intensity maxima and minima appears due to the interferences as the light travels through the laser grooves. As an example, Fig. 5 shows the light intensity obtained when a ZnO:Al surface patterned with parallel scribes is illuminated with a green laser. The position of the different maxima is well duplicated by the equation for the intensity given by a diffraction grating [18] (green line below) but not the relative intensity (red line). In the studied patterns, the predicted envelop curve (blue line) is not observed and the larger maxima is not always at the center. This is attributed to a parabolic shape of the bottom of the grooves instead the square one assumed in the model.

To study the light scattering produced by these ordered structures we resorted to numerical simulations as described in subsection 2.3 and in more detail in [18]. In Fig. 6A the experimental haze factor at 600 nm is compared with the values obtained from numerical simulation using the experimental profiles. As shown, the numerical simulation yields a good approximation to the experimental data, giving weight to the validity of the constructed model. To see how much influence the ordered structure has in the haze factor versus the random surface we deconvoluted the experimental profiles using the Fourier Transform. By choosing the correct frequency and amplitude values we

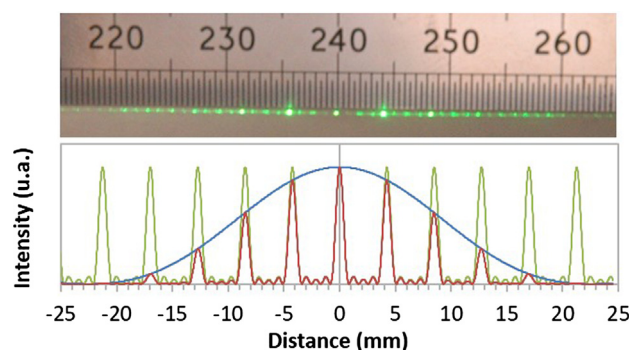


Fig. 5. (Top) Intensity maxima found when illuminating a ZnO:Al film textured with a linear pattern. (Bottom) The position of the maxima are well reproduced by the equation for a diffraction grating (green line) but the relative intensity (red line) differs due to deviations from the theoretical profiles (see text). (For interpretation of the references to colour in this figure legend, the reader is referred to the web version of this article.)

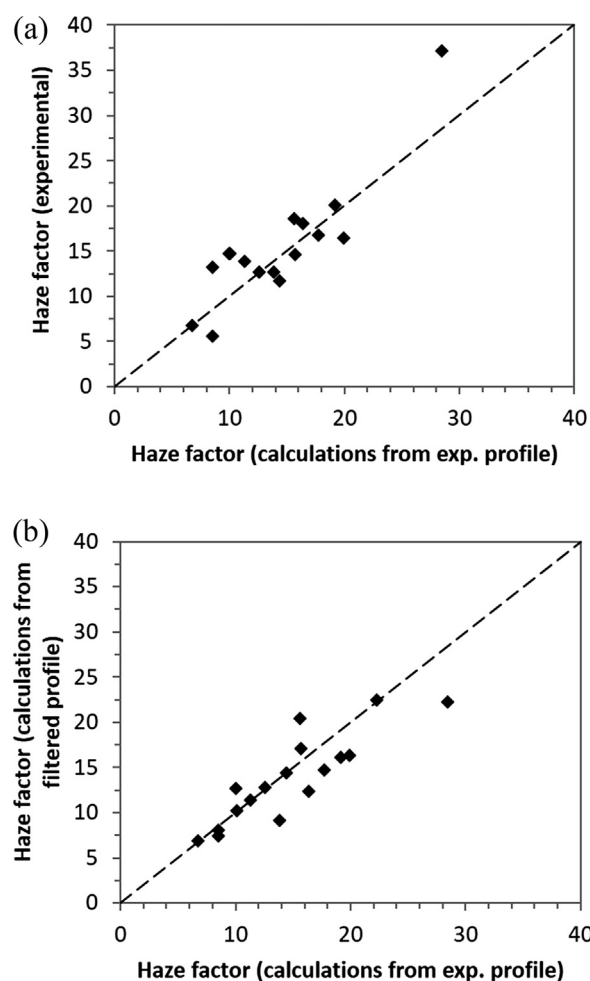


Fig. 6. (A) Haze factor at 600 nm obtained from transmittance spectra versus the haze factor obtained from FEM calculations using the experimental profiles. (B) For the same samples, relationship between the haze factor values calculated using an experimental profile and a filtered profile (See text)). The dashed lines represent the  $Y = X$  situation and are just a guide to the eye.

could discern between the lower frequency/higher amplitude shape of the laser grooves, and the higher frequencies/lower amplitude corresponding to the random roughness. Doing a numerical simulation of the haze factors using the filtered profile for the laser grooves and comparing it to the numerical simulations when using the experimental

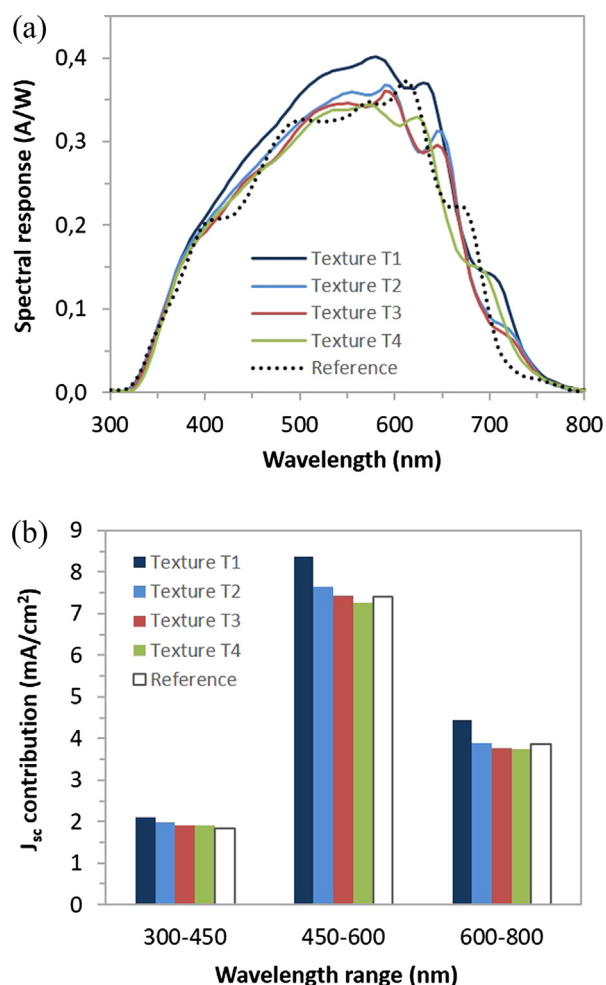


Fig. 7. (A) Spectral response for the solar cells deposited onto the four different ZnO:Al textured substrates (see Fig. 2) and onto as-deposited ZnO:Al. (B) Contribution to  $J_{sc}$  coming from different wavelength ranges for the different solar cells analysed.

profiles (see Fig. 6B) also yields a good correlation, suggesting that most of the light scattering occurs due to the laser scribes rather than the random surface.

### 3.3. Amorphous silicon solar cells

Besides the measurements of the haze factor, a more meaningful test to prove whether the selected substrates can improve the optical behavior of a solar cell under operation is to measure the increase of photon collection within the solar cell. Hence, equivalent solar cells were deposited onto substrates T1-T4 as well as onto a reference, as-deposited ZnO:Al substrate. The measured spectral response of the five different structures is plotted in Fig. 7A. The maxima and minima visible in the reference curve are related to constructive and destructive interferences of the light components perpendicular to the layers interfaces. The light scattering produced by the textured samples softens those maxima and minima, especially up to 600 nm. Texture T1 and, to some extent, texture T2 show an enhancement in the spectral response from 400 nm onwards with respect to the as deposited ZnO:Al substrate.

The improvement observed in the spectral response of the solar cells leads to an increase in  $J_{sc}$  as can be seen in Fig. 7B, where the contribution to  $J_{sc}$  coming from different wavelength ranges is plotted. While the effect in the 300–450 nm range is somewhat limited, both the 450–600 nm and the 600–800 nm ranges present a larger increase in the contribution to  $J_{sc}$ , especially with texture T1.

Table 2

Measured values, and standard deviation, for  $J_{sc}$  in the a-Si:H solar cells deposited onto the different laser-textured AZO films.

	$J_{sc}$ (mA/cm <sup>2</sup> )
Texture 1	14,9 ± 0,06
Texture 2	13,5 ± 0,05
Texture 3	13,1 ± 0,04
Texture 4	12,9 ± 0,04
Reference	13,1 ± 0,05

This increment is also visible in Table 2, where  $J_{sc}$  values for the different textures are collected. While substrates T3 and T4 hardly improve the generated  $J_{sc}$  when compare to the as-deposited ZnO:Al, textures T2 and, especially, T1 produced a boost of 4% (0.5 mA/cm<sup>2</sup>) and 15% (1.9 mA/cm<sup>2</sup>), respectively.

The obtained increment in  $J_{sc}$  of 15% for cells deposited onto T1 is remarkable. As an example, the increase in  $J_{sc}$  seen in a-Si:H solar cells deposited onto Asahi U/AZO TCO textured layers is of 18% when compared to cells where the TCO has been previously polished [21]. Furthermore, this is also a very promising result since the texturing of the films is not optimized and because ZnO:Al has a lower absorption edge than SnO<sub>2</sub>:F due to a smaller band gap, thus partially limiting the effect of the surface morphology. It is also worth noting that in a-Si:H solar cells, light absorption mostly occurs between 300 nm and 800 nm. As the textured samples shown considerable haze factor values at longer wavelengths, some of the effects of the surface morphology are not exploited like it would if other kind of devices, i.e. a tandem a-Si:H/ $\mu$ -Si solar cell, were used instead.

## 4. Conclusions

We have textured RF sputtered ZnO:Al films by direct irradiation with 355 nm nanosecond laser pulses. For simplicity, we have studied only two simple patterns: a linear pattern consisting of parallel grooves equally separated and a crisscross pattern obtained by performing a second array of parallel laser scribes perpendicular to the existing ones. For sufficiently compact patterns with deep scribes, the obtained haze factors reached average values of up to 24% and 34% from 350 nm to 600 nm, and up to 13% and 19% from 600 nm to 900 nm for linear and crisscross patterns respectively.

Two different sources for the light scattering are considered. On the one hand, the surfaces feature a random, low amplitude roughness that accidentally occurs during the scribing process. On the other hand, the scribes that scatter the incident light in a manner similar to a diffraction grating. From numerical simulations using a finite element method and a Fourier transform deconvolution of the surface, we concluded that the laser patterning plays the main role in the scattering of light, opening a field to the use of different geometries to tune the surfaces haze factor

Finally, amorphous silicon solar cells were deposited onto four different textured samples and their spectral response and short-circuit current obtained. The light scattering effect is visible in the reduction of the maxima and minima seen in the spectral response, and lead to an increment in the short-circuit current, especially in the 450–800 nm wavelength range. The substrate with the higher haze factor displayed an increase in short-circuit current of 15% compared to cells deposited onto flat substrates, demonstrating the viability of the proposed approach even though the patterns and the materials chosen were not fully optimized.

## Acknowledgments

The authors would like to thank J. L. Balenzategui for his help in the solar cells characterization. Partial financial support for this work has been provided by the Spanish Ministry of Science and Innovation under

the projects CHENOC (ENE2016-78933-C4-4-R) and HELLO (ENE2013-48629-C4-3-R).

## References

- [1] S. Fernández, J.J. Gandía, Texture optimization process of ZnO: Al thin films using NH<sub>4</sub>Cl aqueous solution for applications as antireflective coating in thin film solar cells, *Thin Solid Films* 520 (2012) 4698–4702.
- [2] I. Olindo, J. Krč, M. Zeman, Modulated surface textures for enhanced light trapping in thin-film silicon solar cells, *Appl. Phys. Lett.* 97 (2010) 101103–101106.
- [3] K.C. Lai, J.H. Wang, C.H. Lu, F.J. Tsai, C.H. Yeh, M.P. Houg, Plasma-induced TCO texture of ZnO: Ga back contacts on silicon thin film solar cells, *Sol. Energy Mater. Sol. Cells* 95 (2011) 415–418.
- [4] M. Vanecek, et al., Nanostructured three-dimensional thin film silicon solar cells with very high efficiency potential, *Appl. Phys. Lett.* 98 (2011) 163503.
- [5] N. Sahraei, K. Forberich, S. Venkataraj, A.G. Aberle, M. Peters, Analytical solution for haze values of aluminium-induced texture (AIT) glass superstrates for a-Si: H solar cells, *Opt. Exp.* 22 (2014) A53–A67.
- [6] L. Zhao, et al., Antireflection silicon structures with hydrophobic property fabricated by three-beam laser interference, *Appl. Surf. Sci.* 346 (2015) 574–579.
- [7] Y.S. Jung, S.S. Lee, Development of indium tin oxide film texture during DC magnetron sputtering deposition, *J. Cryst. Growth* 259 (2003) 343–351.
- [8] J. Dore, et al., Thin-film polycrystalline silicon solar cells formed by diode laser crystallisation, *Prog. Photovoltaics Res. Appl.* 21 (2012) 1377–1383.
- [9] M.D. Abbott, J. Cotter, Optical and electrical properties of laser texturing for high-efficiency solar cells, *Prog. Photovolt Res. Appl.* 14 (2006) 225–235.
- [10] V. Blattmann, D. Trusheim, Hybrid laser-etching-process for wafer texturing, *Energy Procedia* 77 (2015) 766–773.
- [11] M. Sanz, E. Rebolgar, R. a. Ganeev, M. Castillejo, Nanosecond laser-induced periodic surface structures on wide band-gap semiconductors, *Appl. Surf. Sci.* 278 (2013) 325–329.
- [12] M. Soldera, K. Taretto, J. Berger, A.F. Lasagni, Potential of photocurrent improvement in  $\mu\text{c-Si: H}$  solar cells with TCO substrates structured by direct laser interference patterning, *Adv. Eng. Mater.* 18 (9) (2016) 1674–1682.
- [13] J. Berger, T. Roch, S. Correia, J. Eberhardt, A.F. Lasagni, Controlling the optical performance of transparent conducting oxides using direct laser interference patterning, *Thin Solid Films* 612 (2016) 342–349.
- [14] E.V. Johnson, P. Prodhomme, C. Boniface, K. Huet, T. Emeraud, P. Roca I Cabarrocas, Excimer laser annealing and chemical texturing of ZnO: Al sputtered at room temperature for photovoltaic applications, *Sol. Energy Mater. Sol. Cells* 95 (2011) 2823–2830.
- [15] B. Li, L. Huang, N. Ren, X. Kong, Y. Cai, J. Zhang, Two-step preparation of laser-textured Ni/FTO bilayer composite films with high photoelectric properties, *J. Alloys Compd.* 640 (2015) 376–382.
- [16] V. Jovanov, et al., Influence of interface morphologies on amorphous silicon thin film solar cells prepared on randomly textured substrates, *Sol. Energy Mater. Sol. Cells* 112 (2013) 182–189.
- [17] J.D. Santos, S. Fernández, J. Cárabe, J.J. Gandía, Cause of the fill factor loss of a-Si: H p-i-n devices with ZnO: Al front electrode: Blocking contact vs. Defect density, *Thin Solid Films* 548 (2013) 617–622.
- [18] D. Canteli, et al., Analysis by finite element calculations of light scattering in laser-textured AZO films for PV thin-film Solar cells, *Energy Procedia* 84 (2015) 78–85.
- [19] J. Krč, M. Zeman, O. Kluth, F. Smole, M. Topič, Effect of surface roughness of ZnO: Al films on light scattering in hydrogenated amorphous silicon solar cells, *Thin Solid Films* 426 (2003) 296–304.
- [20] M. Zeman, R.A.C.M.M. van Swaaij, J.W. Metselaar, R.E.I. Schropp, Optical modeling of a-Si: H solar cells with rough interfaces: effect of back contact and interface roughness, *J. Appl. Phys.* 88 (2000) 6436–6443.
- [21] M. Van Lare, F. Lenzmann, A. Polman, M. van Lare, F. Lenzmann, A. Polman, Dielectric back scattering patterns for light trapping in thin-film Si solar cells, *Opt. Exp.* 21 (18) (2013) 20738–20746.